

Label-free density difference amplification-based cell sorting

Jihwan Song,^{1,a)} Minsun Song,^{2,a)} Taewook Kang,^{2,3,b)} Dongchoul Kim,^{1,b)} and Luke P. Lee^{2,b)}

¹*Department of Mechanical Engineering, Sogang University, Seoul 121-742, Korea*

²*Departments of Bioengineering, Electrical Engineering and Computer Science, and Biophysics Program, University of California at Berkeley, Berkeley, California 94720, USA*

³*Department of Chemical and Biomolecular Engineering, Sogang University, Seoul 121-742, Korea*

(Received 9 August 2014; accepted 13 November 2014; published online 26 November 2014)

The selective cell separation is a critical step in fundamental life sciences, translational medicine, biotechnology, and energy harvesting. Conventional cell separation methods are fluorescent activated cell sorting and magnetic-activated cell sorting based on fluorescent probes and magnetic particles on cell surfaces. Label-free cell separation methods such as Raman-activated cell sorting, electro-physiologically activated cell sorting, dielectric-activated cell sorting, or inertial microfluidic cell sorting are, however, limited when separating cells of the same kind or cells with similar sizes and dielectric properties, as well as similar electrophysiological phenotypes. Here we report a label-free density difference amplification-based cell sorting (dDACS) without using any external optical, magnetic, electrical forces, or fluidic activations. The conceptual microfluidic design consists of an inlet, hydraulic jump cavity, and multiple outlets. Incoming particles experience gravity, buoyancy, and drag forces in the separation chamber. The height and distance that each particle can reach in the chamber are different and depend on its density, thus allowing for the separation of particles into multiple outlets. The separation behavior of the particles, based on the ratio of the channel heights of the inlet and chamber and Reynolds number has been systematically studied. Numerical simulation reveals that the difference between the heights of only lighter particles with densities close to that of water increases with increasing the ratio of the channel heights, while decreasing Reynolds number can amplify the difference in the heights between the particles considered irrespective of their densities.

© 2014 AIP Publishing LLC. [<http://dx.doi.org/10.1063/1.4902906>]

Separating specific cells from heterogeneous or homogeneous mixtures has been considered as a key step in a wide variety of applications ranging from biomedicine to energy harvesting. For example, the separation and sorting of rare circulating tumor cells (CTCs) from whole blood has gained significant importance in the potential diagnosis and treatment of metastatic cancers.^{1,2} Similarly, malaria detection relies on the collection of infected red blood cells (RBCs) from whole blood.^{3,4} In addition, the selective separation of lipid-rich microalgae from homogeneous mixtures of microalgae is a promising technique in biomass conversion.⁵

To date, conventional cell separation can be done by labelling cells with biomolecules to induce differences in physical properties. For instance, in a fluorescence-activated cell sorter (FACS), cells to be separated are labelled with antibodies or aptamers with fluorescent molecules, and then sorted by applying an electrical potential.^{6,7} Similarly, magnetic-activated cell sorter (MACS) uses magnetic.^{8,9} Alternatively, label-free cell separation methods have exploited inherent

^{a)}J. Song and M. Song contributed equally to this work.

^{b)}Authors to whom correspondence should be addressed. Electronic addresses: twkang@sogang.ac.kr; dckim@sogang.ac.kr; and lplee@berkeley.edu

differences in the physical properties (e.g., size and dielectric properties) of different kinds of cells. For example, acoustophoresis forces particles larger than a desired size to move into the center of a fluidic channel by using ultrasonic standing waves.^{10–12} Inertial microfluidics takes advantage of curved fluidic channels in order to amplify the size differences between particles.^{13,14} Mass-dependent separation of particles based on gravity and hydrodynamic flow was also reported.¹⁵ Particles with different dielectric properties can also be sorted by dielectrophoresis which induces the movement of polarizable particles.^{16–18}

The disadvantage of these methods, however, is that they require external forces and labels that may cause unexpected damage to biological cells.^{19–21} More importantly, most methods are limited in separating cells of the same kind or cells with similar sizes and dielectric properties.

Here we designed a novel, label-free density difference amplification-based cell sorting (dDACS) that allows the separation of particles with the same size and charge by exploiting subtle differences in density without the use of external forces. Figure 1(a) illustrates the proposed microfluidic model and its underlying mechanism. The conceptual microfluidic system consists of an inlet, a separation chamber (hydraulic jump cavity), and multiple outlets. Particles entering through the inlet experience gravity (F_G), buoyancy (F_B), and drag (F_D) forces in the separation chamber. The net force acting on the particles can be described as

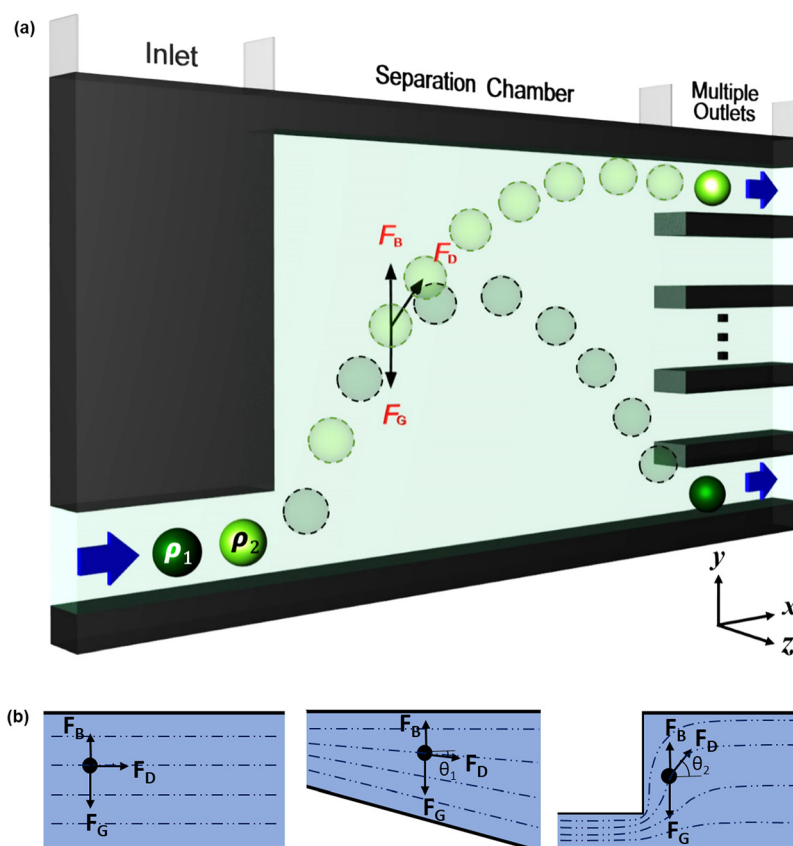


FIG. 1. Schematic illustration of label-free density difference amplification-based cell sorting (dDACS), which exploits differences in the densities ($\rho_1 > \rho_2$) of particles with similar diameters (d) and charge. (a) The conceptual microfluidic design consists of an inlet, a separation chamber (hydraulic jump cavity), and multiple outlets. Incoming particles experience gravity (F_G), buoyancy (F_B), and drag (F_D) forces in the separation chamber, and depending on their densities, the height (H) and distance (D) that each particle is able to reach will be different, allowing the particles to be separated into multiple outlets. (b) Possible microfluidic channel configurations for density-based separation: Uniform channel height (left), gradual channel expansion (middle), and hydraulic jump cavity with sudden channel expansion (right). The height difference between particles with different densities can be amplified by the sudden channel expansion compared to the other two cases due to the relatively large tangential angle, θ of F_D . ($|\theta_1| \ll |\theta_2|$) (see Fig. S1 in the supplementary material²²).

$$F = F_G + F_B + F_D. \quad (1)$$

As particles enter the separation chamber (i.e., hydraulic jump cavity), F_D acting on the particles changes its direction along the streamline. The particles experience additional forces in the y direction due to large tangential angle (Fig. 1(b)). For lighter particles, whose densities are close to that of the surrounding water, F_D becomes comparable to F_G (i.e., in the y direction), while the net force for heavier particles is less affected by this additional contribution of F_D due to a large F_G . As a result, the height (H) and distance (D) that each particle can travel are different depending on its density. The difference in the maximum height (ΔH_{\max}) between two particles with different density (ρ_{p1} and ρ_{p2}) can be further approximated as

$$\Delta H_{\max} \propto \frac{(v_{yp0})^2}{(v_{yf} - v_{yp0})}, \quad (\rho_{p1} - \rho_{p2}), \quad (2)$$

where v_{yp0} and v_{yf} represent the velocity of particle and fluid along the y direction at the entrance of hydraulic jump cavity, respectively.

In comparison with the other two cases (Fig. 1(b) uniform channel height and gradual channel expansion), the height difference between the particles with different densities can be amplified by the sudden channel expansion in the hydraulic jump cavity due to relatively large tangential angle (see supplementary material²²). Therefore, the particles can be separated through the multiple outlets, depending on their height and distance.

In order to analyze the separation behavior of particles in the chamber according to differences in their densities, H and D are systematically investigated. The numerical simulations are performed using a commercial CFD software (CFX 14.0; ANSYS 14.0; ANSYS, Inc.). Particles with the same density may have different trajectories in the separation chamber depending on their inlet positions (Fig. 2(a)). Prior to this investigation, the maximum height (H_{\max}) and distance (D_{\max}) for each particle are compared by examining H and D of 100 identical particles at different inlet positions since the inlet position of particles could be controlled.²⁰ Fig. 2(b) shows H_{\max} and D_{\max} of particles with respect to density at a fixed Reynolds number ($Re = 0.1$). Note that Reynolds number is defined as $Re = \rho_f v_f D_h / \mu$, where ρ_f , v_f , D_h , μ are density of fluid, velocity of the fluid, hydraulic diameter of a channel, and dynamic viscosity of the

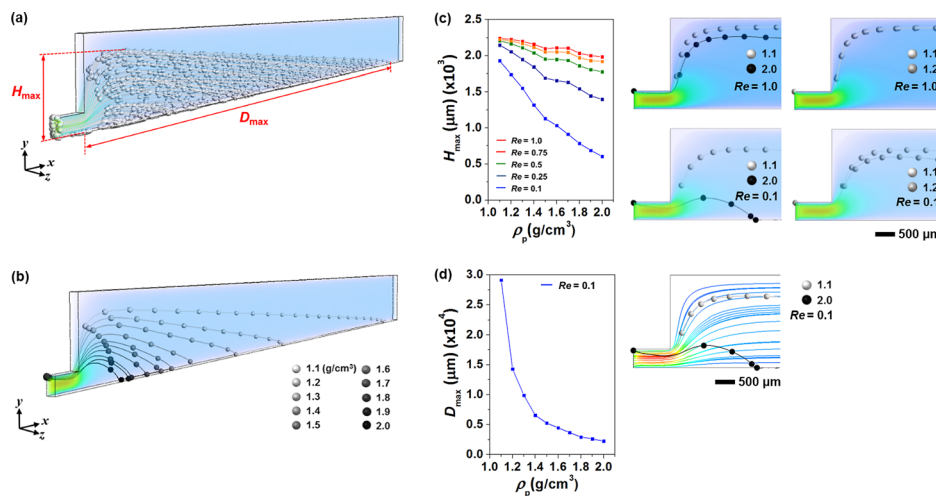


FIG. 2. Microfluidic particle separation with respect to Reynolds number (Re). (a) Trajectories in the separation chamber of a hundred particles with the same density starting from inlet positions chosen arbitrarily in order to investigate the effect of the inlet positions on the maxima of the height (H_{\max}) and distance (D_{\max}) prior to further simulation. (b) Representative trajectories of particles having different densities from 1.1 to 2.0 g/cm³. (c) The maximum height (H_{\max}) of each particle with respect to Re . (d) Representative maximum distance (D_{\max}) of each particle at $Re = 0.1$. (Left) Streamline of fluid and representative trajectories of particles with densities of 1.1 and 2.0 g/cm³ in the separation chamber at $Re = 0.1$ (right).

fluid, respectively. The hydraulic diameter in the Reynolds number is determined with the inlet channel. Particle densities in the range of 1.1 to 2.0 g/cm³ are chosen with the increase of 0.1 g/cm³. These values are quite reasonable in that the densities of many microorganisms such as microalgae are typically within this range and their densities can be varied by 0.2 g/m³ depending on their cellular context.²³ The lighter particles travel with a higher H_{\max} , and longer D_{\max} . With the separation chamber, the height difference between particles with densities of 1.1 and 1.2 g/cm³ can be amplified by about 10 times as compared to that in a channel without the chamber, judging from the position where the 1.1 g/cm³ particle reaches its H_{\max} .

In Fig. 2(c), the values for H_{\max} of particles with respect to Reynolds number (Re) are presented. Since in our study, the maximum height (H_{\max}) and distance (D_{\max}) for each particle were compared by examining H and D of 100 identical particles that are randomly distributed in the channel (throughout all figures), there is little variation in H_{\max} and D_{\max} between each simulation. However, the standard deviation between each simulation is quite small and can be negligible. The H_{\max} values particles at $Re = 0.5$ with densities of 1.1 g/cm³ and 1.2 g/cm³ are $2.21 \times 10^3 \mu\text{m}$ and $2.17 \times 10^3 \mu\text{m}$, respectively. The difference between H_{\max} of different particles, ΔH_{\max} , increases with decreasing Re . For example, ΔH_{\max} between particles with densities of 1.1 and 2.0 g/cm³ becomes $0.26 \times 10^3 \mu\text{m}$ at $Re = 1.0$, but increases to $1.38 \times 10^3 \mu\text{m}$ as Re decreases to 0.1. As Re increases (velocity of fluid increases), the relative velocity in the y direction between the fluid and the particle increases resulting in increasing of F_D in the y direction since the velocity of particle in the y direction is very small at the entrance of the separation chamber. Thus, contribution of F_D becomes comparable to the net force in the y direction. As a result, most of the particles even in the case of heavier ones travel quite similarly with the streamline, and ΔH_{\max} subsequently decreases. On the other hand, as Re decreases, the contribution of F_G becomes dominant due to the decrease of F_D in the y direction. Consequently, the particles start to cross downwards streamlines as the density of the particles increases and H_{\max} gradually decreases. In addition, irrespective of their densities, ΔH_{\max} of the particles increases with decreasing Re .

Fig. 2(d) shows D_{\max} with respect to the density of the particles (left). Different densities of particles show different trajectories due to the relative contribution of F_D to the net force in the y direction depending on the particle density (right). At $Re = 0.1$, D_{\max} of particles with densities of 1.1 g/cm³ and 1.2 g/cm³ are $2.91 \times 10^4 \mu\text{m}$ and $1.43 \times 10^4 \mu\text{m}$, respectively. As the density of a particle increases, its D_{\max} dramatically decreases. The difference in D_{\max} between particles with densities of 1.1 and 1.2 g/cm³ is $1.48 \times 10^4 \mu\text{m}$, and $0.0037 \times 10^4 \mu\text{m}$ for particles with densities of 1.9 and 2.0 g/cm³. The effect of F_D is stronger compared to that of F_G on lighter particles. Thus, lighter particles travel quite similarly with the streamline and finally have a large D_{\max} . On the other hand, heavier particles where effect of F_G is stronger compared to that of F_D cross downwards streamlines and finally have a small D_{\max} .

Next, in order to investigate the separation behavior of particles with respect to the geometry of the microfluidic device, the effect of the ratio of the height of the separation chamber (h_c) to the inlet (h_i) on H_{\max} is investigated as shown in Fig. 3. Interestingly, H_{\max} of particles with density of 1.1 g/cm³ increases from $1.93 \times 10^3 \mu\text{m}$ to $6.48 \times 10^3 \mu\text{m}$ while that of particles with density of 1.9 g/cm³ slightly changes from $0.70 \times 10^3 \mu\text{m}$ to $0.73 \times 10^3 \mu\text{m}$ as h_c/h_i increases from 5 to 20.

This result can be attributed to two effects: (1) the change in the streamline and (2) the relative contribution of drag force to the net force depending on the density. With increasing h_c/h_i , dramatic increase in H_{\max} for lighter particles is because the streamline for the lighter ones experiences more vertical displacement in the separation chamber and the contribution of F_D to the net force acting on the lighter one is more significant (see Fig. S2 in the supplementary material²²).

Based on this approach, we propose a microfluidic device for the selective separation of the lightest particle. Fig. 4(a) shows one unit (with three outlets) of the proposed microfluidic device that can be connected in series. The ratio of channel heights (h_c/h_i) is set to 20, and the particle densities are in the range of 1.1 ~ 1.5 g/m³. Fig. 4(b) shows the representative separation behavior of the particles. A portion of the lightest particles (1.1 g/cm³) is selectively

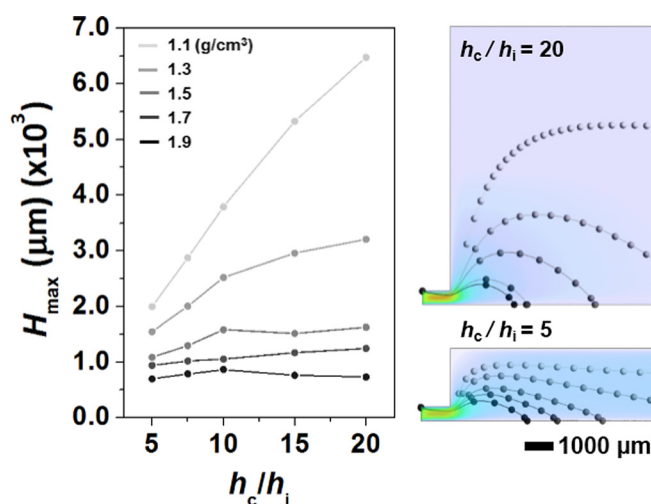


FIG. 3. Microfluidic particle separation with respect to the ratio of the height of the inlet (h_i) to the separation chamber (h_c).

separated into the upper and middle outlets, while remaining light particles together with four other heavier particles with densities in the range of 1.2 to 1.5 g/cm³ leave through the lowest outlet. With a single operation of this unit, 40% of the lightest particles are recovered. In addition, the yield increases with increasing number of cycles (Fig. 4(c)).

In summary, we have demonstrated a label-free microfluidic system for the separation of particles according to subtle differences in their densities without external forces. Our microfluidic design consists simply of an inlet, a separation chamber, and multiple outlets. When entering the separation chamber, the particles experience an additional drag force in the y direction, amplifying the difference in both the height and the distance that the particles with different

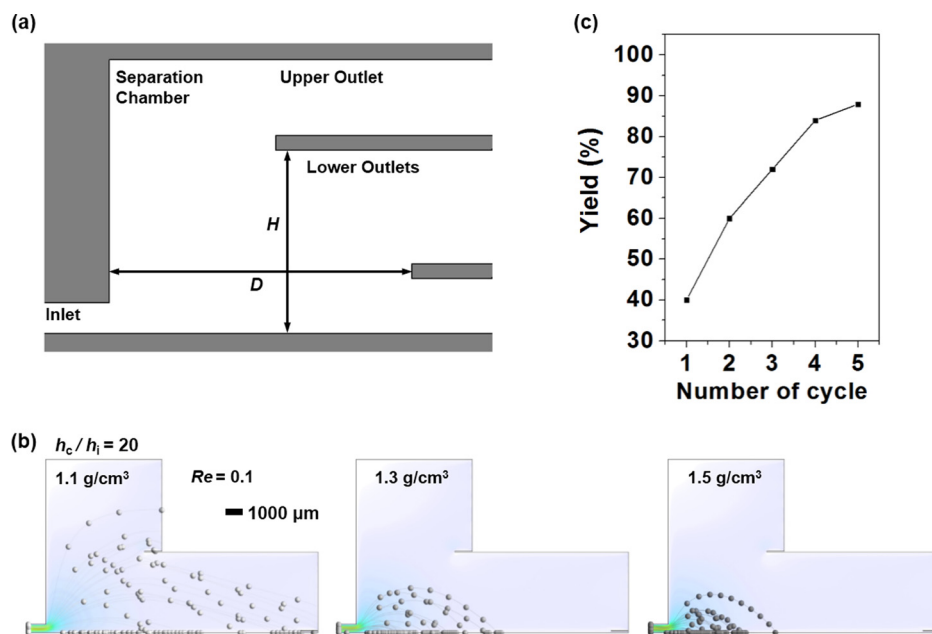


FIG. 4. (a) One unit of the proposed microfluidic device for the selective separation of the lightest particle based on the simulation results. Particles are separated into two outlets based on differences in both the height and distance travelled stemming from differences in density. (b) Representative separation behavior of particles observed in the device. (c) The yield of the lightest particle (1.1 g/cm³) with the proposed microfluidic device according to the number of cycles (i.e., this unit is assumed to be connected in series).

densities can travel within the chamber. At a fixed Reynolds number, with increasing particle density, H_{\max} decreases monotonously, and D_{\max} decreases dramatically. On the other hand, as Reynolds number increases, the difference between the heights of particles with different densities is attenuated. In addition, the simulation reveals that increasing the ratio of the channel heights increases the difference between the heights of particles only when their densities are close to that of the surrounding water. Based on this approach, a microfluidic device for the separation of the lightest particles has been proposed. We expect that our density-based separation design can be beneficial to the selective separation of specific microorganisms such as lipid-rich microalgae for energy harvesting application.

This work was supported by Korea CCS R&D Center (KCRC) grant funded by the Korea government (Ministry of Science, ICT & Future Planning) (Grant No. 2013M1A8A1056301), the Basic Science Research Program through the National Research Foundation of Korea (NRF) funded by the Ministry of Science, ICT and Future Planning (Grant No. NRF-2013R1A1A2011263), the International Research & Development Program of the National Research Foundation of Korea (NRF) funded by the Ministry of Science, ICT & Future Planning (Grant No. 2013K1A3A1A32035444), and Leading Foreign Research Institute Recruitment Program through the National Research Foundation of Korea (NRF) funded by the Ministry of Science, ICT and Future Planning (MSIP) (Grant No. 2013K1A4A3055268).

- ¹N. M. Karabacak, P. S. Spuhler, F. Fachin, E. J. Lim, V. Pai, E. Ozkumur, J. M. Martel, N. Kojic, K. Smith, P. Chen, J. Yang, H. Hwang, B. Morgan, J. Trautwein, T. A. Barber, S. L. Stott, S. Maheswaran, R. Kapur, D. A. Haber, and M. Toner, *Nat. Protoc.* **9**, 694 (2014).
- ²H. W. Hou, M. E. Warkiani, B. L. Khoo, Z. R. Li, R. A. Soo, D. S. Tan, W. Lim, J. Han, A. A. S. Bhagat, and C. T. Lim, *Sci. Rep.* **3**, 1259 (2013).
- ³P. Gascoyne, C. Mahidol, M. Ruchirawat, J. Satayavivad, P. Watcharasit, and F. Becker, *Lab Chip*, **2**, 70 (2002).
- ⁴P. Gascoyne, J. Satayavivad, and M. Ruchirawat, *Acta Tropica* **89**, 357 (2004).
- ⁵A. W. D. Larkum, I. L. Ross, O. Kruse, and B. Hankamer, *Trends Biotechnol.* **30**, 198 (2012).
- ⁶G. Mayer, M. S. L. Ahmed, A. Dolf, E. Endl, P. A. Knolle, and M. Famulok, *Nat. Prot.* **5**, 1993 (2010).
- ⁷M. M. Wang, E. Tu, D. E. Raymond, J. M. Yang, H. Zhang, N. Hagen, B. Dees, E. M. Mercer, A. H. Forster, I. Kariv, P. J. Marchand, and W. F. Butler, *Nat. Biotechnol.* **23**, 83 (2005).
- ⁸J. D. Adams, U. Kim, and H. T. Soh, *PNAS*, **105**, 18165 (2008).
- ⁹K. Schriebl, G. Satianegara, A. Hwang, H. L. Tan, W. J. Fong, H. H. Yang, A. Jungbauer, and A. Choo, *Tissue Eng. Part A* **18**, 899 (2012).
- ¹⁰Y. Liu and K. M. Lim, *Lab Chip* **11**, 3167 (2011).
- ¹¹N. R. Harris, M. Hill, S. Beeby, Y. Shen, N. M. White, J. J. Hawkes, and W. T. Coakley, *Sens. Actuators B* **95**, 425 (2003).
- ¹²M. Evander, A. Lenshof, T. Laurell, and J. Nilsson, *Anal. Chem.* **80**, 5178 (2008).
- ¹³S. S. Kuntaegowdanahalli, A. A. S. Bhagat, G. Kumar, and I. Papautsky, *Lab Chip* **9**, 2973 (2009).
- ¹⁴D. C. Dino, *Lab Chip*, **9**, 3038 (2009).
- ¹⁵D. Huh, J. H. Bahng, Y. Ling, H. H. Wei, O. D. Kripfgans, J. B. Fowlkes, J. B. Grotberg, and S. Takayama, *Anal. Chem.* **79**, 1369 (2007).
- ¹⁶M. D. Vahey and J. Voldman, *Anal. Chem.* **80**, 3135 (2008).
- ¹⁷U. Kim, J. R. Qian, S. A. Kenrick, P. S. Daugherty, and H. T. Soh, *Anal. Chem.* **80**, 8656 (2008).
- ¹⁸X. Y. Hu, P. H. Bessette, J. R. Qian, C. D. Meinhart, P. S. Daugherty, and H. T. Soh, *Proc. Natl. Acad. Sci. U.S.A.* **102**, 15757 (2005).
- ¹⁹P. Sajeesh and A. K. Sen, *Microfluid. Nanofluid.* **17**, 1 (2014).
- ²⁰T. Morijiri, S. Sunahiro, M. Senaha, M. Yamada, and M. Seki, *Microfluid. Nanofluid.* **11**, 105 (2011).
- ²¹A. A. S. Bhagat, H. Bow, H. W. Hou, S. J. Tan, J. Han, and C. T. Lim, *Med. Biol. Eng. Comput.* **48**, 999 (2010).
- ²²See supplementary material at <http://dx.doi.org/10.1063/1.4902906> for calculation details.
- ²³E. Eroglu and A. Melis, *Biotechnol. Bioeng.* **102**, 1406 (2009).